Geophysical Investigation of Pavement Failure in a Basement Complex Terrain of Southwestern Nigeria.

O.J. Akintorinwa, Ph.D.[1*]; J.S. Ojo, Ph.D.[1]; and M.O. Olorunfemi, Ph.D. [2]

[1]Department of Applied Geophysics, Federal University of Technology, Akure, Nigeria.
[2]Department of Geology, Obafemi Awolowo University, Ile-Ife, Nigeria.

E-mail: orllyola@yahoo.com*

ABSTRACT

Geophysical investigation was carried out along segments of the Ilesa-Akure highway located in the Precambrian Basement Complex of Southwestern Nigeria with a view to establishing the cause(s) of the road pavement failure. Four failed segments and two stable segments serving as control were studied. The magnetic and the Very Low Frequency Electromagnetic (VLF-EM) measurements were taken at intervals of 5 m along traverses established parallel to road pavement. The Vertical Electrical Sounding (VES) involving the Schlumberger array and 2-D imaging using the dipole-dipole configuration were adopted for the resistivity survey.

The magnetic and VLF-EM results revealed that the control stable segments are founded on a near homogeneous substratum devoid of major geological features while anomalies typical of linear features suspected to be fault/fractured zones and lithological boundaries were identified within the failed localities. The geoelectric sections generally identified four geologic layers comprising the topsoil, weathered layer, partly weathered/fractured basement and fresh bedrock. The subsoils on which the road pavement was founded at control stable segments have moderate to high resistivity values (>200 Ω-m) while the subsoils on which the failed segments are founded are of relatively low resistivity values that are generally less than 200 Ω-m. Network of suspected linear (geological) structures such as fractures and faults were identified from the 2-D resistivity structure across the failed segments.

The causes of highway pavement failure in the studied highway may have been clayey topsoil/sub-grade soils with characteristically low resistivity values of < 200 Ω–m and near-surface linear features such as faults, fractures and lithologcal contacts beneath the highway pavements.

(Keywords: geophysical investigation, pavement failure, basement complex terrain)

INTRODUCTION

Road transportation is an important element in the physical development of any society as it controls the direction and extent of development (Bolaji, 2003). Good roads promote the economic growth of a nation by creating enabling environment for the movement of goods and services. Oil and gas products, solid minerals, raw and finished products are moved to points of need via roads. A good network of roads will reduce haulage vehicle accidents thereby minimizing human and material losses.

The failure of highway in Nigeria, especially those constructed after the independence in 1960, has been of great concern. Inspite of various rehabilitation efforts several segments of our highway still fail perpetually. Much of the nation's resources that could have been channeled into the provision of educational, health and other social facilities are expended on rehabilitation of roadways. Such rehabilitation has become an annual ritual and a big financial burden on various tiers of government. Road failures are not limited to any particular geologic setting. Failures have been recorded on both the crystalline Basement Complex rocks and Sedimentary Formations.

The Ilesa-Akure highway (Figure 1), which was constructed in 1978, serves as a major link from the southwest to the northern and eastern parts of the country. Ten failed segments of the highway (Figure 2) have experienced perpetual failure after rehabilitations.

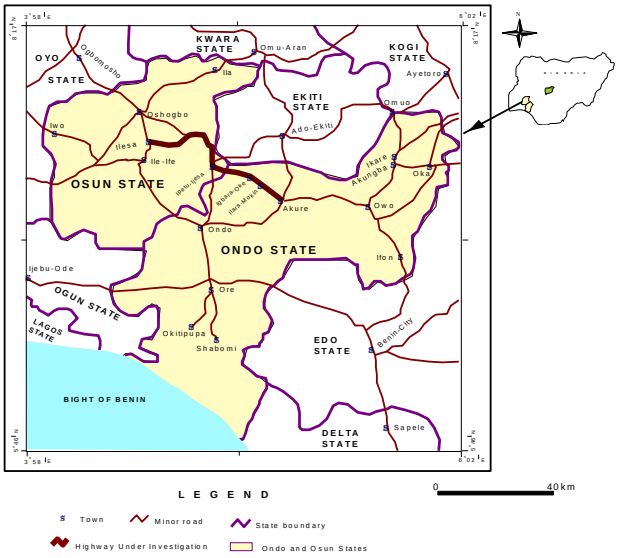

Figure 1: Road Map of Part of Southwestern Nigeria Showing the Ilesa–Akure Highway. (Modified After Spectrum Road Map, 2002)

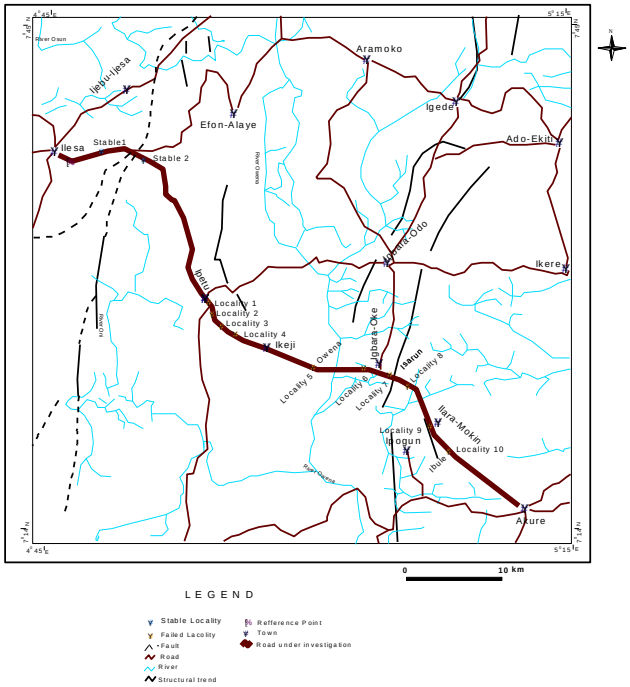

Figure 2: Map of the Area around Ilesa-Akure Highway Showing the Specific Sites Studied.

The pattern of failure-pitting, rutting, cracking and pothole which had taken place along the highway can be broadly attributed to any or a combination of geological, geotechnical, design, construction and usage problem. However, both the stable and failed segments of the highway fall within the same broad geological setting (Basement Complex) and have the same design, construction and usage capacity. It is, therefore, suspected that other factors may be responsible. The need to establish these other factors has necessitated this study.

Description of the Studied Highway

The Ilesa-Akure highway is about 70km long (Figure 1). It traverses Osun and Ondo States. The highway lies within latitudes 7^0 14' N and 7^0 45' N and longitudes 4^0 45' E and 5^0 15' E (Figure 1).

Expressed in the Universal Traverse Mercator (UTM) coordinates of Zone 31 using Minna datum, the highway is located within Northings 0800084mN and 0857239mN and Eastings 0693225mE and 0748163mE. The topography along the highway is gently undulating. The highway is located within the tropical climatic region.

The region experiences two seasons- the dry and wet (rainy) seasons (Iloeje, 1981). The rainy season starts during the months of March – April and lasts till around October. The mean annual rainfall ranges between 1270 and 1524 mm (Federal Survey, 1978). The relative humidity is about 60%-85% from November to March, and about 80%-90% around August. The mean temperature varies between 27^0C and 31^0C. According to the Federal Survey (1978), the area lies in the rain forest. The vegetation is dense and made up of broad-leaved trees that are mostly evergreen.

Geology of the Area along the Studied Highway

The geological map in the area around the Ilesa-Akure highway is shown in Figure 3. The highway cuts across six rock units namely migmatite, basic schist undifferentiated, granite-gneiss, quartz-schist and quartzite, porphyritic granite and charnockite.

METHOD OF STUDY

Four major failed segments (Locality 1, 5, 7, and 10; Figure 2) straddling different geomphlogical

features, varied lithological units and ranging in length from 350–500m and the two stable segments were studied. The geophysical investigation involved the electromagnetic, electrical resistivity and magnetic methods. One traverse was established at each of the localities parallel to the road pavement, and was made to cut across the stable (as at the time of investigation) and the failed segment of the highway. A typical field layout is shown in Figure 4.

Magnetic Survey

Magnetic, measurements were made at 5m interval along each of the traverses with the GSM 8 Proton Precession Magnetometer (PPM). Two magnetic measurements with sensor height at 1.5m, were taken per station and the mean of the magnetic measurements adopted for each observed station.

A set of readings was taken at an established base station close to each traverse before the commencement and immediately after data acquisition. The base station readings were used for diurnal and offset corrections. Corrected magnetic data were plotted against station positions.

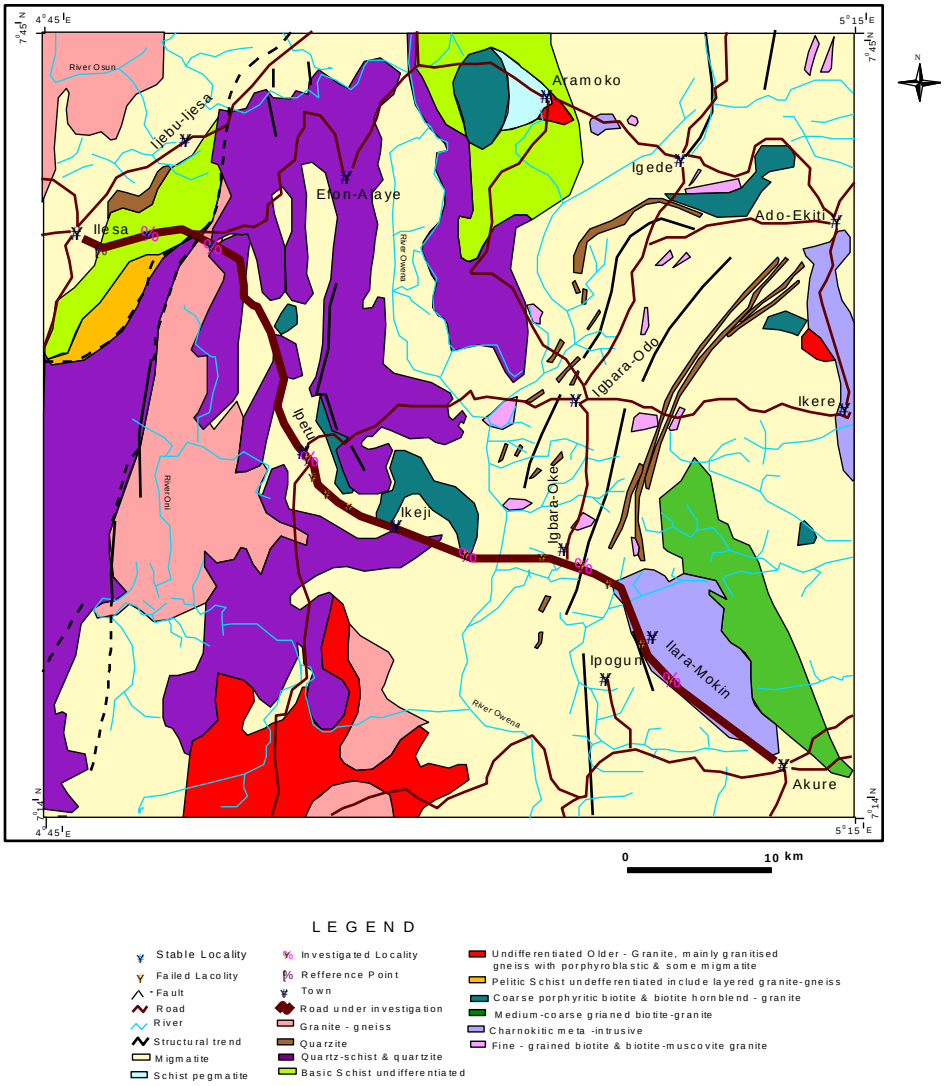

Figure 3: Geological Map of the Area around Ilesa-Akure Showing the Ilesa-Akure Highway (Modified After Geological Survey of Nigeria, 1976).

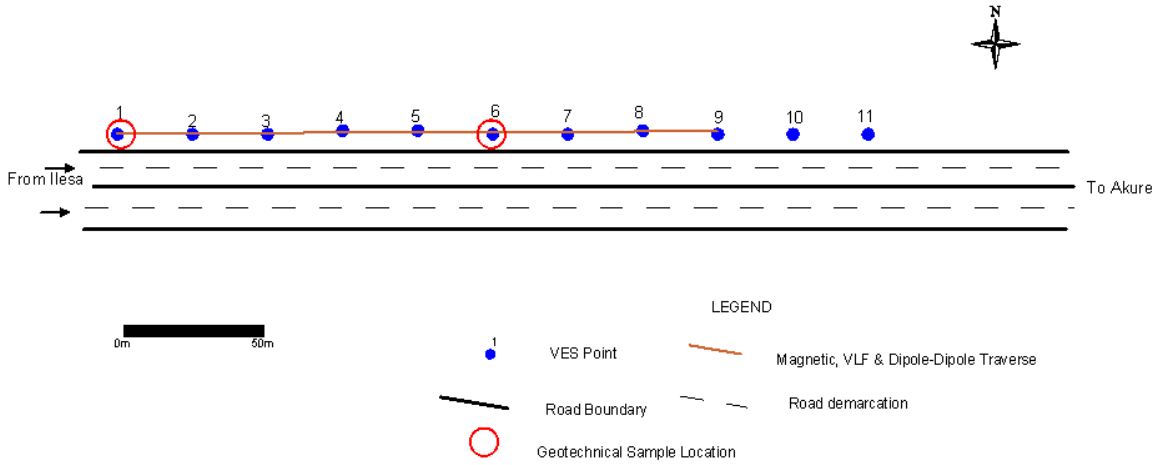

Figure 4: Typical Field Layout.

VLF-EM Survey

The Very Low Frequency Electromagnetic (VLF – EM) method utilized the inline profiling technique. VLF-EM measurements were also taken at 5 m interval along each traverse with Geonics EM 16 VLF. The real and quadrature components of the vertical/horizontal magnetic field ratio were recorded at each observation station. The receiver unit was tuned to Rugby in Great Britain. The real and filtered real (Karous and Hjeit, 1983) components were plotted against station positions using 'KHFFILT' software version 1.1a. A 2-D inversion of the real component data was carried out using the same software.

Electrical Resistivity Survey

The electrical resistivity method utilized two field techniques - Vertical Electrical Sounding (VES) involving the Schlumberger array and 2-D electrical imaging using dipole-dipole configuration. Sounding stations were established at 25 m interval. Twenty-two (22) sounding stations were occupied along the control stable segments, while Seventy-seven (77) sounding stations were occupied along the failed segments. The current electrode spacing (AB/2) was varied from 1 m to 65 m.

The apparent resistivity measurements were plotted against electrode spacing on bi-logarithmic graph sheets. Partial curve matching was carried out for the quantitative interpretation of the sounding curves. The results of the curve matching (layer resistivities and thicknesses) were used as starting model parameters for 1-D forward modeling using RESIST version 1.0 (Vander Velper, 1988). The VES interpretation results were used for the construction of geoelectric sections along the various segments.

2-D Electrical Imaging

2-D resistivity data acquisition was carried out with the dipole-dipole array (Alpin, 1966). The inter-electrode spacing of 5m was adopted while inter-dipole expansion factor (n) was varied from 1 to 5. The apparent resistivity values were presented as pseudosections. 2-D inversion of the dipole-dipole data was carried out using the DIPRO for Windows (2001) software.

RESULTS AND DISCUSION

Tables 1-6 give a summary of the interpretation results of the VES curves at each of the studied localities. The number of layers varies between 3 and 6. Eight curve types have been identified in all the locations. These include the A, H, HA, HK, KH, QH, HKH, and KHKH type. The histogram of the curve types from stable 1 and stable 2 and those from the failed segments 1, 5, 7, and 10 are shown in Figures 5a and 5b, respectively.

Table 1: VES Interpretation Results from Stable Segment 1.

VES NO	RESISTIVITY (ρ) (Ω-m)					THICKNESS (h) (m)				CURVE TYPE
	ρ_1	ρ_2	ρ_3	ρ_4	ρ_5	h_1	h_2	h_3	h_4	
1	163	791	144	635	-	0.6	0.9	4.3	-	KH
2	869	394	1132	-	-	0.9	7.4	-	-	H
3	1294	7956	2209	∞	-	0.8	1.3	22.6	-	KH
4	2511	1573	3443	-	-	0.8	2.7	-	-	H
5	2573	690	1641	691	∞	0.5	1.8	4.1	11.4	HKH
6	956	320	∞	-	-	1.0	11.3	-	-	H
7	1080	782	311	∞	-	1.5	5.0	14.6	-	QH
8	185	92	583	-	-	0.7	2.0	-	-	H
9	500	400	675	1625	-	0.9	1.7	14.7	-	HA
10	1262	185	1070	-	-	0.7	3.9	-	-	H
11	969	214	661	-	-	1.0	5.7	-	-	H

Table 2: VES Interpretation Results from Stable Segment 2.

VES NO	RESISTIVITY (ρ) (Ω-m)				THICKNESS (h) (m)			CURVE TYPE
	P_1	ρ_2	ρ_3	ρ_4	h_1	H_2	h_3	
12	1005	1194	278	1422	0.7	2.1	4.6	KH
13	729	961	441	1775	1.0	3.6	17.6	KH
14	1358	383	6914	-	2.3	14.8	-	H
15	1387	363	2273	-	2.0	12.9	-	H
16	2078	432	2048	-	1.8	8.2	-	H
17	2139	361	∞	-	1.9	9.7	-	H
18	2028	351	∞	-	2.1	9.4	-	H
19	3306	437	∞	-	1.4	11.6	-	H
20	3344	445	∞	-	1.5	14.6	-	H
21	2407	352	6306	-	1.9	9.6	-	H
22	3780	547	3329	-	1.4	8.7	-	H

Table 3: VES Interpretation Results from Locality 1.

VES NO	RESISTIVITY (ρ) (Ω-m)				THICKNESS (h) (m)			CURVE TYPE
	ρ_1	ρ_2	P_3	P_4	h_1	h_2	h_3	H
23	772	103	2463		1.1	6.6		H
24	717	76	7830		1.6	5.4		H
25	501	85	5555		1.6	5.0		H
26	329	63	2930		1.5	5.7		H
27	643	76	∞		2.1	7.9		H
28	660	130	794		1.4	3.9		H
29	298	40	∞		0.9	6.3		H
30	425	76	∞		1.0	5.9		H
31	344	33	1266		1.1	2.3		H
32	246	37	∞		1.1	3.1		H
33	283	34	∞		1.5	3.8		H
34	484	23	∞		1.2	3.4		H
35	373	33	∞		1.4	4.8		H
36	543	53	∞		1.2	4.9		H
37	1405	108	2722		0.9	7.5		H
38	730	134	7956		0.8	9.0		H
39	155	107	162	∞	0.8	0.9	12.3	HA
40	829	101	3915		0.8	4.0		H
41	480	240	∞		0.8	8.0		H
42	300	108	∞		1.0	6.6		H
43	597	134	∞		0.9	10.3		H
44	342	82	2097		1.0	7.2		H

Table 4: VES Interpretation Results from Locality 5.

VES NO	RESISTIVITY (ρ) (Ω-m)				THICKNESS (h) (m)			CURVE TYPE
	ρ_1	ρ_2	ρ_3	ρ_4	h_1	h_2	h_3	
45	438	2216	359	∞	0.9	1.6	41.9	KH
46	541	1282	173	∞	1.0	2.7	16.4	KH
47	525	292	239	∞	0.9	1.2	16.0	KH
48	1137	1327	244	∞	1.0	1.8	15.8	KH
49	1039	134	∞		2.1	13.2		H
50	1121	207	∞		1.2	1.7		H
51	1357	150	∞		1.1	10.4		H
52	205	339	154	∞	1.1	2.5	7.3	KH
53	950	190	2700		1.4	7.4		H
54	560	364	3700		1.2	4.3		H
55	480	782	465	1857	0.8	1.4	2.9	KH
56	845	626	∞		1.2	9.1		H
57	411	214	∞		1.3	6.5		H
58	338	210	399	∞	0.8	0.7	12.7	HA
59	459	92	2012		1.1	5.6		H
60	390	51	∞		1.1	2.8		H
61	656	101	∞		1.5	5.5		H
62	392	46	∞		1.5	2.9		H
63	420	168	∞		1.5	10.5		H
64	414	437	2483		1.0	10.9		A
65	388	461	9086		1.2	2.9		A
66	234	244	4394		0.9	1.7		A

Table 5: VES Interpretation Results from Locality 7.

VES NO	RESISTIVITY (ρ) (Ω-m)						THICKNESS (h) (m)					CURVE TYPE
	ρ_1	ρ_2	ρ_3	ρ_4	ρ_5	P_6	H_1	h_2	h_3	H_4	h_5	
67	432	119	∞				1.2	6.1				H
68	516	238	∞				1.8	6.4				H
69	445	61	∞				1.5	4.1				H
70	505	31	∞				2.2	4.9				H
71	316	139	3410				1.9	12.7				H
72	252	122	∞				1.9	4.5				H
73	295	185	371	∞			1.1	3.1	8.0			HA
74	221	694	76	1683			0.7	0.5	1.5			KH
75	348	106	872				0.8	3.6				H
76	419	679	370	∞			0.5	0.3	1.2			KH
77	416	268	593	989			1.0	0.8	8.9			HA
78	477	432	1459				0.9	.09				H
79	997	588	∞				1.6	2.8				H
80	650	329	840	553			0.9	0.9	16.0			HK
81	719	593	1299	658	932		1.0	1.2	0.9	2.4		HKH
82	894	502	889				0.6	3.9				H
83	852	916	597	1880	653	1859	0.8	1.0	1.6	4.2	20.7	KHKH

Table 6: VES Interpretation Results from Locality 10.

VES NO	RESISTIVITY (ρ) (Ω-m)				THICKNESS (h) (m)			CURVE TYPE
	ρ_1	ρ_2	ρ_3	ρ_4	h_1	h_2	h_3	
84	178	22	∞		1.2	9.9		H
85	12	09	∞		1.5	5.9		H
86	46	09	∞		1.7	7.1		H
87	59	09	∞		2.1	7.7		H
88	70	24	60	2179	0.8	1.3	17.4	HA
89	261	23	192		1.3	3.1		H
90	30	15	1478		1.0	1.6		H
91	38	46	987		0.8	11.9		H
92	108	27	127		1.1	3.7		H
93	62	47	252		0.9	3.5		H
94	120	48	550		1.0	6.2		H
95	84	52	251		1.3	11.8		H
96	237	66	1457		0.5	10.6		H
97	126	33	36	377	0.6	0.9	3.5	HA
98	111	61	154	299	0.8	1.8	6.6	HA
99	234	63	259		0.5	2.7		H

The two histograms show a predominant H type curve. This implies that curve types may not be good indicators of stability of highway pavement since the stable section and failed section display predominantly the same curve types.

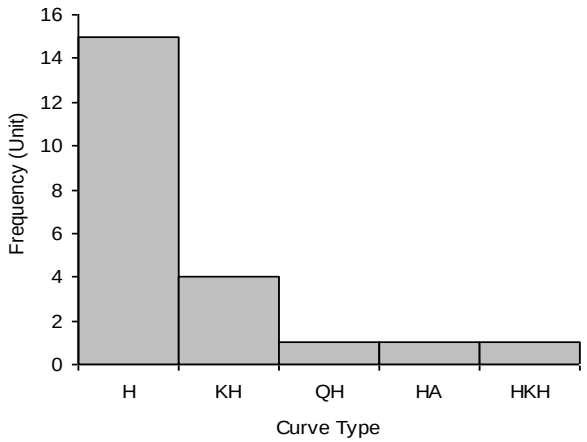

Figure 5a: Histogram of the Curve Type in the Stable 1 and 2.

The stable segment 1 is characterized by relatively high resistivity topsoil and weathered layer in the upper 0-5 m with resistivity values that are generally greater than 200 Ω-m (Table 1).

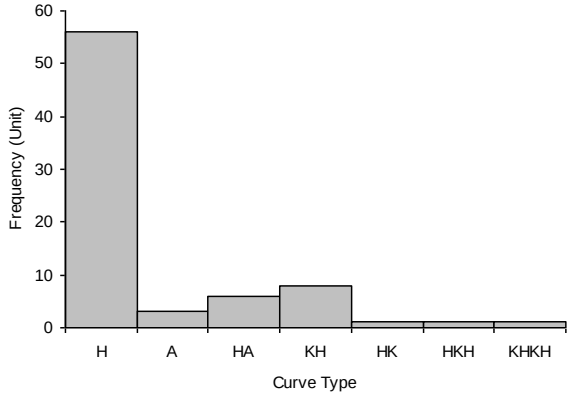

Figure 5b: Histogram of the Curve Types at Localities 1, 5, 7 and 10.

The subsoil layer is composed of clayey sand and laterite (Figure 6a). The major magnetic anomaly (Figure 6b) observed at this locality is due to a resistive magnetized basement intrusion whose top is located at around 80 m (Figure 6c) where the basement rock outcrops (Figure 6a and Figure 6d). The VLF-EM 2-D model (Figure 6c) identifies this magnetic body as a poorly conductive target.

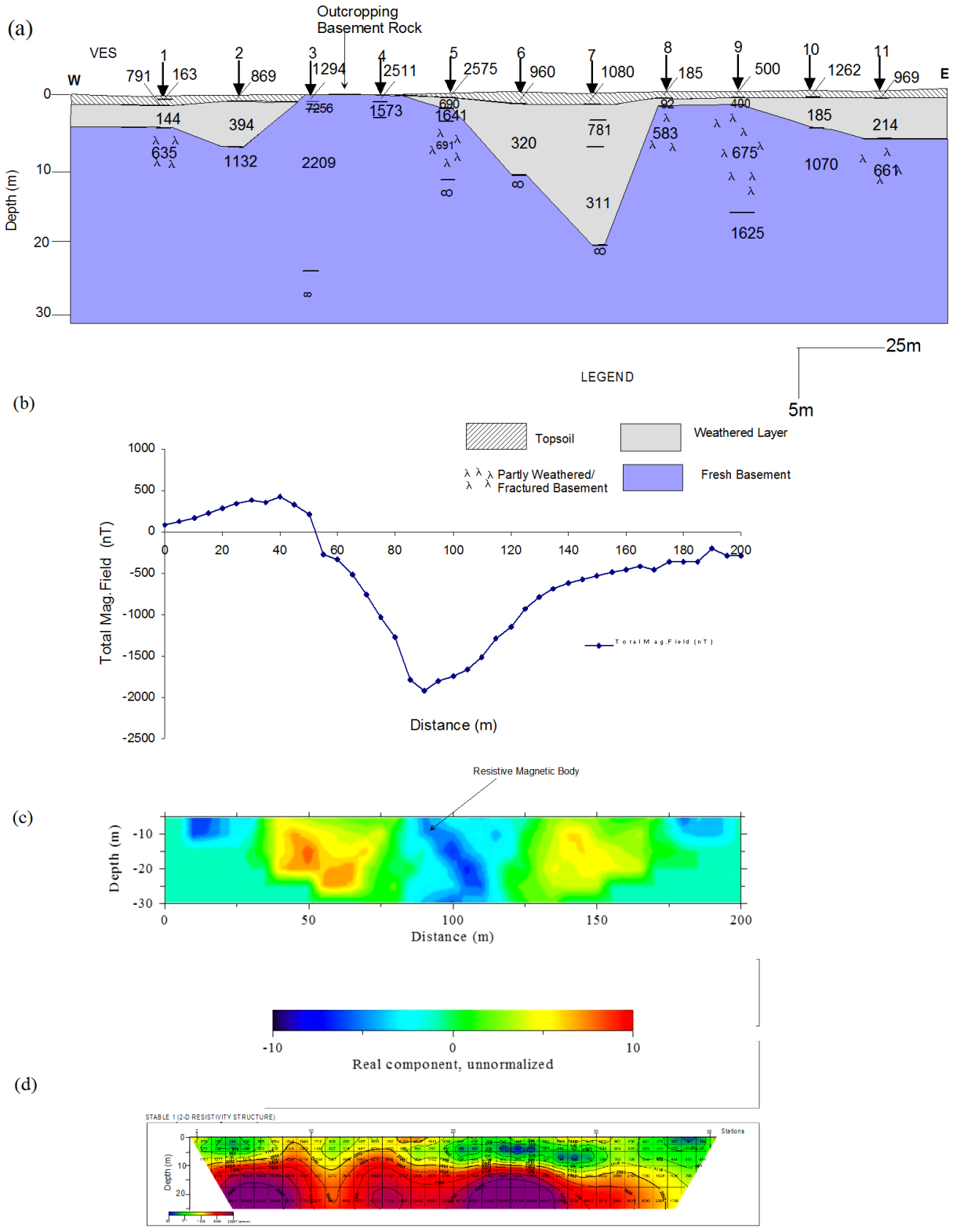

Figure 6: (a) Geoelectric Section, (b) Magnetic Profile, (c) 2-D VLF Inversion Model and (d) 2-D Dipole-Dipole Resistivity Structure at Stable Segment 1.

The stable segment 2 is characterized by lateritic formation in the upper 2-3 m with resistivity values varying from 728 to 3780 Ω-m (Table 2). The underlying weathered layer is composed of clayey sand with resistivity values ranging from 278 to 547 Ω-m (7a). The relatively flat magnetic profile along this segment (Figure 7b) and a VLF-EM inverted model (Figure 7c) that is devoid of linear feature are indications of a near homogeneous subsurface sequence (Figure 7d).

The control stable segments therefore have the following characteristics:

(i) The road pavements are founded on topsoil/subsoil with moderate to high layer resistivity values (>200 Ω-m) and whose composition ranges from clayey sand to laterite with sandy clay in places.

(ii) The segments are generally devoid of linear geological features such as fractures, faults, lithological contact etc., which are zones of weakness that may increase porosity and fluid permeability of the subsoil and hence decrease the load bearing capacity of the road pavement.

At failed locality 1 (Figure 8a), both the topsoil and the subsoil (weathered layer) in the upper 0-8 m are clayey within the failed and the presently classified stable segments at the flanks with resistivity values generally less than 100 Ω-m (Table 3). The basement relief is uneven (Figure 8a and Figure 8d). Both the magnetic profile (Figure 8b) and the 2-D resistivity structures (Figure 8d) identify suspected linear features within the failed segment at distances 165, 255, 275m and 310 m and within the currently classified stable segment at distances 45 and 425 m.

Some of these linear features display fairly high conductivity on the VLF-EM 2-D model (Figure 8c). The identified linear features have significant depth extent (>5 m) which may indicate geological features such as fractures and faults. Road pavement failure at this locality may have been precipitated by a combination of an incompetent clayey subsoil and network of near-surface and subsurface linear features suspected to be lithological contact or fault/fracture zones.

Locality 5 (Figure 9a) has sandy clay/clayey sand and laterite in the upper 0.8-2.1 m with resistivity values generally grater than 200 Ω-m (Table 4). The underlying weathered layer is predominantly sandy clay/clayey sand within the failed and the presently classified stable segments at the flanks with resistivity values generally grater than 200 Ω-m (Figure 9a). The basement relief is uneven (Figure 9a and Figure 9d). The magnetic profile (Figure 9b) and the 2-D resistivity structure (Figure 9d) identify suspected linear features within the failed segment at 185 m, 310 m and 370 m and the presently classified stable segment at 70 m and 490 m.

Some of these linear features show fairly high conductivity on the VLF-EM 2-D model (Figure 9c). All the identified linear features have significant depth extent (> 7 m) and this may indicate geological features, such as fractures, faults and lithological contacts. Failure at the locality 5 may have been due to network of near-surface and subsurface linear features suspected to be lithological contact, fault/fracture zone.

Both the topsoil and the weathered layer in the upper 0-8 m at the northwestern flank of locality 7 is composed of clay, sandy clay and clayey sand beneath the failed and the currently classified stable segments at the flanks with resistivity values generally less than 200 Ω-m (Figure 10a). The southeastern flank has a relatively thin overburden (maximum 1.6 m) and it is composed of clayey sand and laterite with resistivity values generally greater than 200 Ω-m (Table 5).

The basement bedrock interface is uneven and dipping toward the northwest (Figure 10a and Figure 10d). A linear feature suspected to be a fault or lithological contact is located at distance of 140 m on the 2-D resistivity structure (Figure 10d). This feature was also delineated by the VLF-EM 2-D model (Figure 10c) and magnetic anomaly (Figure 10b).

A suspected confined basement fracture is located between distance of 215m and 260m on the 2-D resistivity structure (Figure 10d), which falls within an intensively fractured basement bedrock zone delineated between distance of 225m and 400m on the geoelectric section (Figure 10a). These identified linear features fall within the magnetic anomaly located between distance of 150m and 360m on the magnetic profile (Fig. 10b). All the identified linear features have significant depth extent and falls within the failed and the presently classified stable segments.

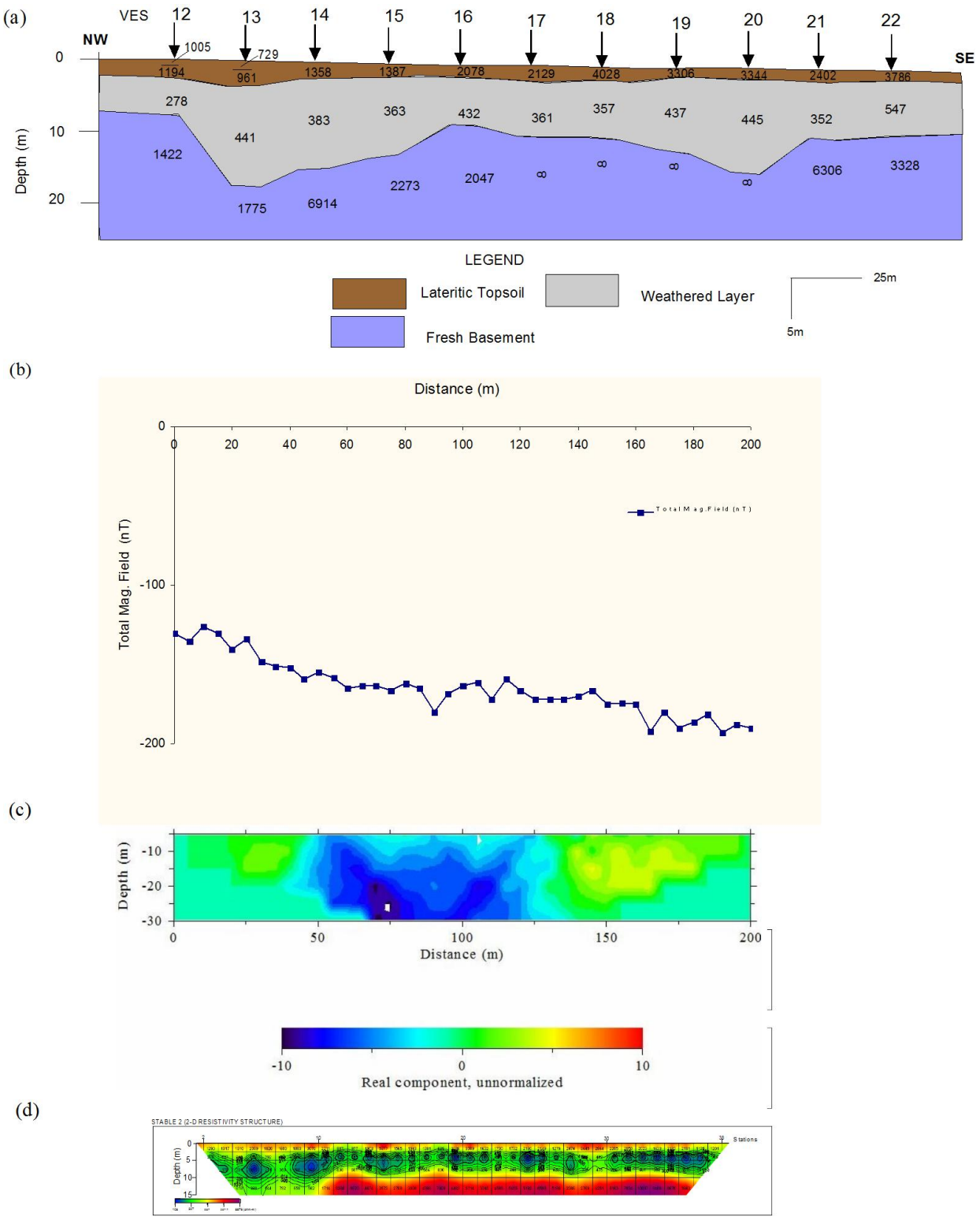

Figure 7: (a) Geoelectric Section, (b) Magnetic Profile, (c) 2-D VLF Inversion Model and (d) 2-D Dipole-Dipole Resistivity Structure at Stable Segment 2

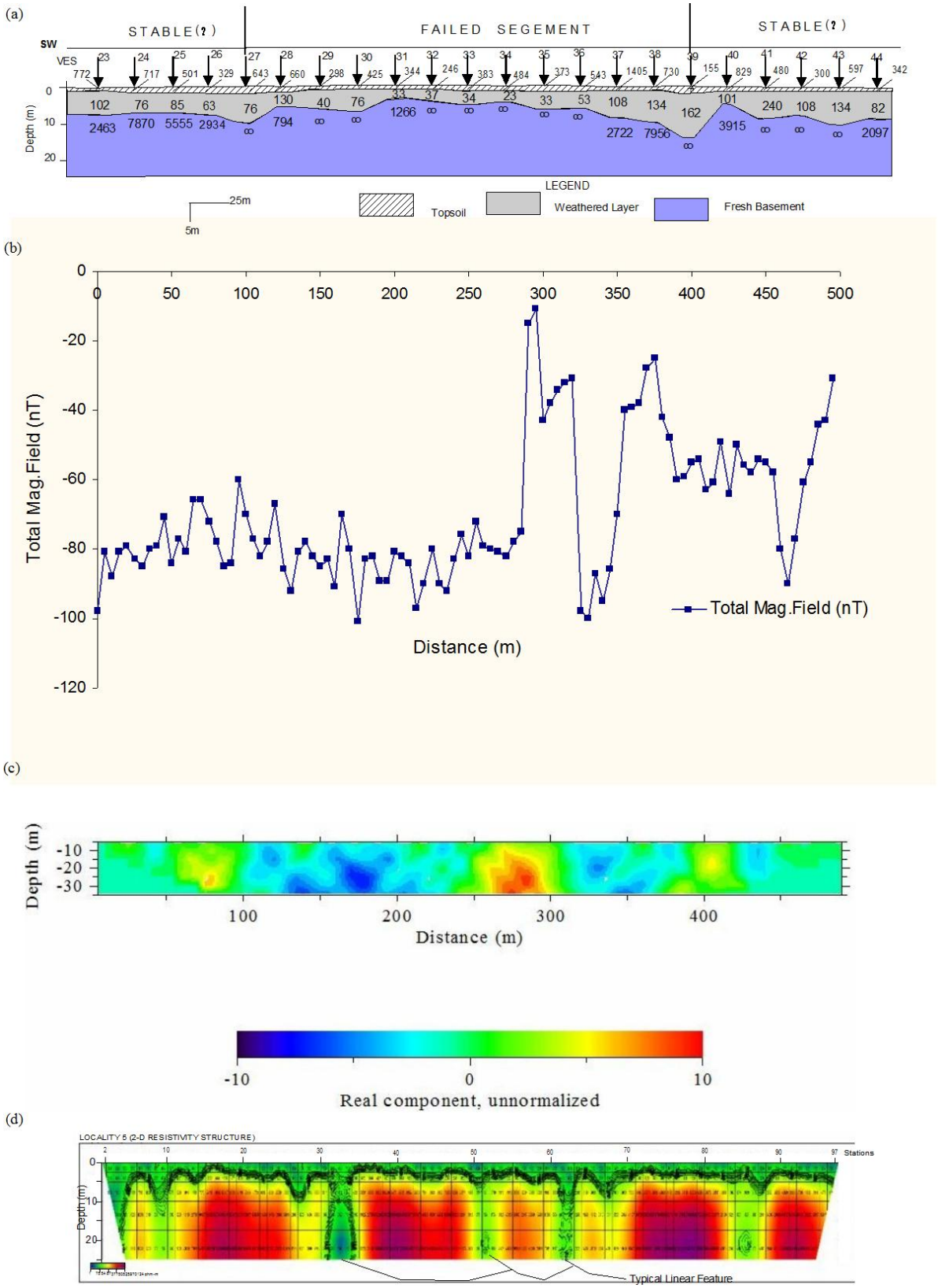

Figure 8: (a) Geoelectric Section, (b) Magnetic Profile, (c) 2-D VLF Inversion Model and (d) 2-D Dipole-Dipole Resistivity Structure at Locality 1.

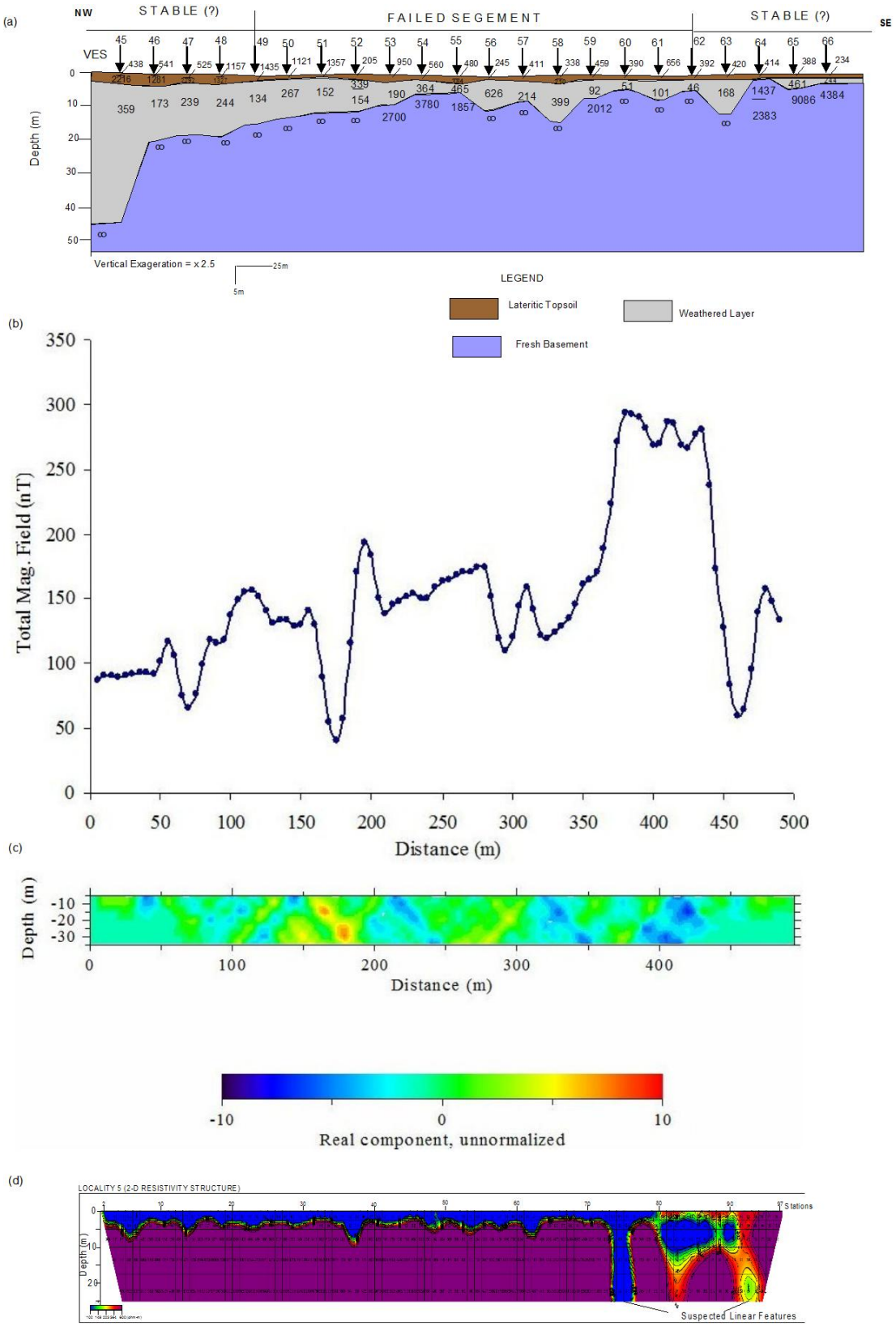

Figure 9: (a) Geoelectric Section, (b) Magnetic Profile, (c) 2-D VLF Inversion Model and (d) 2-D Dipole-Dipole Resistivity Structure at Locality 5.

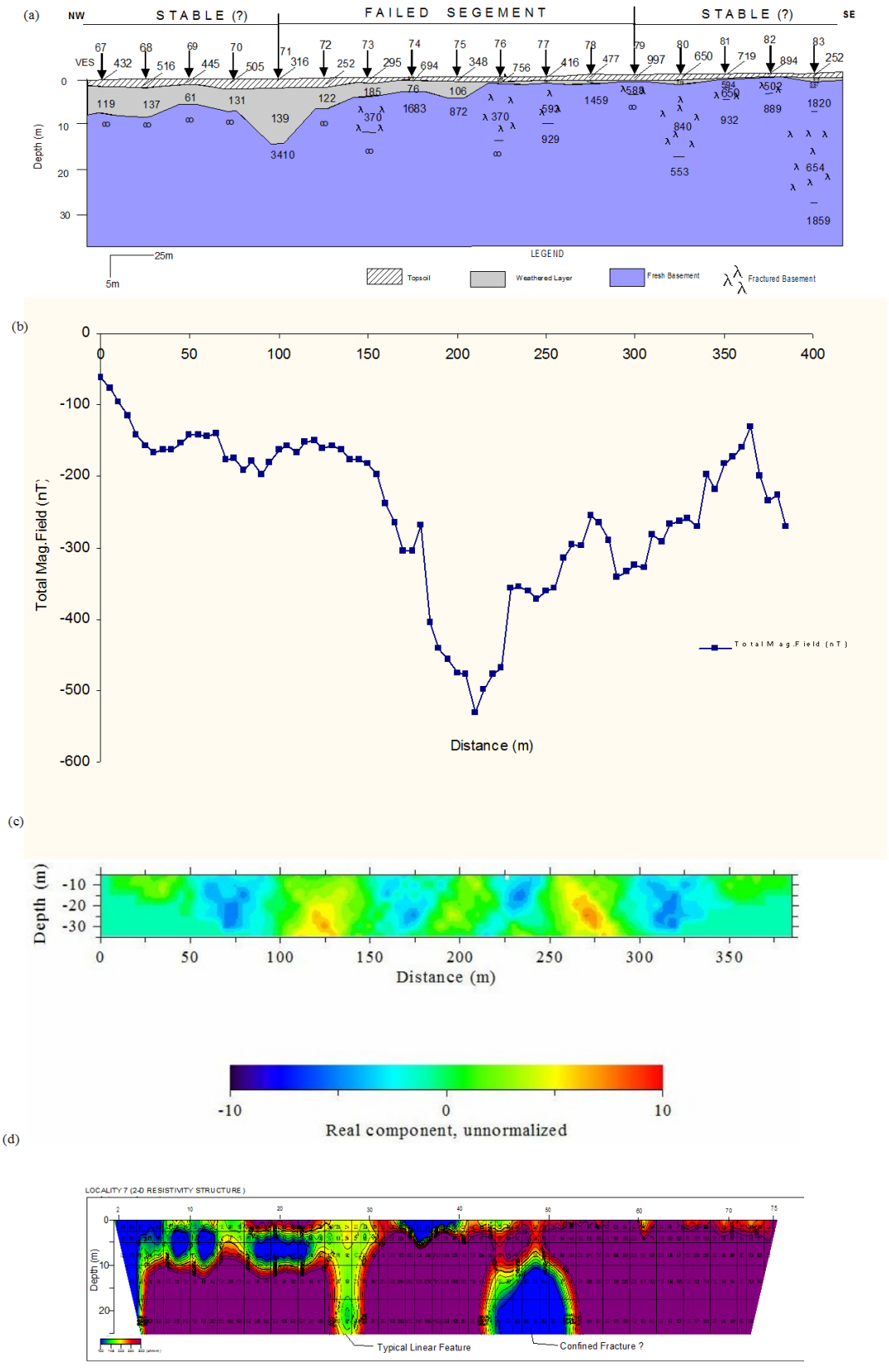

Figure 10: (a) Geoelectric Section, (b) Magnetic Profile, (c) 2-D VLF Inversion Model and (d) 2-D Dipole-Dipole Resistivity Structure at Locality 7.

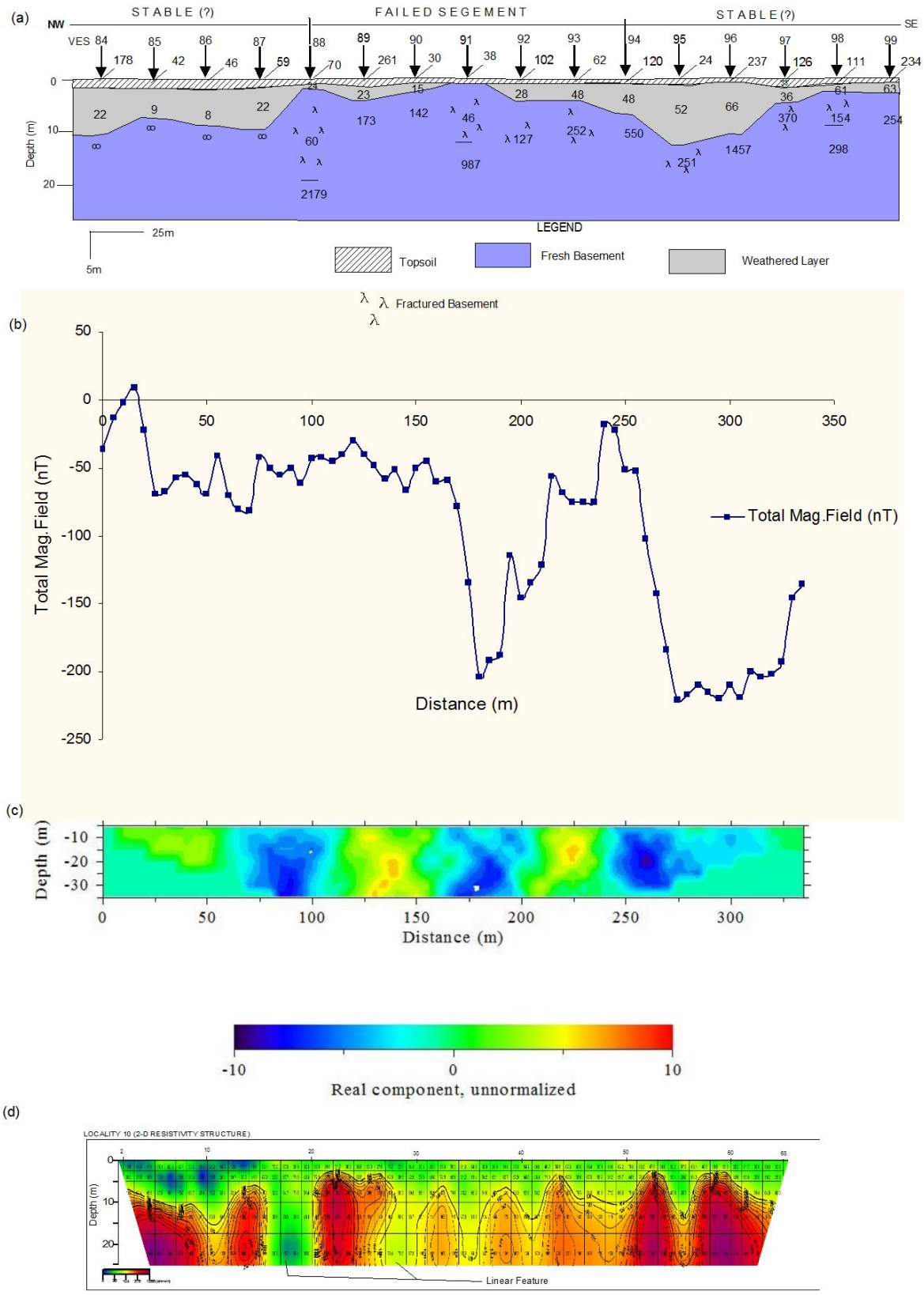

Figure 11: (a) Geoelectric Section, (b) Magnetic Profile, (c) 2-D VLF Inversion Model and (d) 2-D Dipole-Dipole Resistivity Structure at Locality 10.

Failure at locality 7 may have been precipitated by incompetent clayey subsoil on the northwestern flank and network of near-surface and sub surface linear features suspected to be lithological contact or fault/fracture zones on the southeastern flanks.

At locality 10 (Fig. 11a), the topsoil and the weathered layer within the failed and the currently classified stable segment flanks are composed of clay which is up to 10 m thick. The resistivity values are generally less than 100 Ω-m (Table 6).

The basement bedrock topography is uneven (Figure 11a and Figure 11d). The 2-D resistivity structure (Figure 11d) identify suspected linear features within the failed segment at distances of 145 m and 175 m and within the "stable" segment at distances 90 m and 275 m. Some of these linear features show fairly high conductivity on the VLF-EM 2-D inversion model (Figure 11c).

The identified linear features have significant depth extent (> 12 m) and may indicate geological features such as fractures/faults and lithological contacts. Failure at this locality may have been precipitated by a combination of an incompetent clayey subsoil and network of near-surface and subsurface linear features suspected to be faults/ fracture zones.

CONCLUSIONS

It can be concluded from the study that, the possible causes of pavement failure along the studied highway are:

(i) Clayey topsoil/sub-grade soils with characteristics low layer resistivity of less than 100 Ω–m. The soil type absorbs water, swells and collapses under imposed traffic load stress and thereby leading to pavement failure.

(ii) Near-surface linear (geological) features such as faults, fractures and lithologcal contacts beneath the highway pavements. These features act as zones of weakness that enhances the accumulation of water leading to pavements failure.

To confirm the above, the classified stable sections on both flanks of the failed segments at most of the localities investigated, particularly at localities 1 and 10, whose pavements were founded on incompetent (clay) subsoil and within whose segments linear features were delineated, failed before the conclusion of this study.

REFERENCES

1. Alpin, L.M. 1966. *The Theory of Dipole Sounding in Dipole Methods for Measuring Earth Conductivity*. Consult Bureau: New York, NY. 1-60.

2. Bolaji, A.A. 2003. "Highway Geotechnical Properties of Soils in Some Sections of Ibadan-Ilorin Road, Nigeria". Unpublished B.Sc Dissertation Dept. of Civil Engineering, Lautech Ogbomoso, Nigeria.

3. Dipro for Windows. 2001. "DiproTM Version 4.0.1, Processing and Interpretation Software for Electrical Resistivity Data". KIGAM: Daejon, South Korea.

4. Federal Survey. 1978. *Atlas of the Federal Republic of Nigeria, 1st Edition*. Federal Surveys: Lagos, Nigeria. 136.

5. Geological Survey of Nigeria. 1976. *Geological Map of Ilesa, Akure, Ondo and Ado-Ekiti*. GSN: Lagos, Nigeria.

6. Iloeje, N.P. 1981. *A New Geography of Nigeria (New Revised Edition)*. Longman Nig. Ltd.: Lagos, Nigeria. 201.

7. Karous, M.R. and Hjelt, S.E. 1983. "Linear Filtering of VLF Dip Angle Measurements". *Geophysical Prospecting*. 31:782-794.

8. KHFFILT. 2004. *Karous-Hjelt and Fraser Filtering of VLF Measurements, Version 1.1a*. Markku Pirttijarvi.

9. Vander Velper, B.P.A. 1988. "Resist Version 1.0". M.Sc. Research Project, ITC, Delf Netherland.

SUGGESTED CITATION

Akintorinwa, O.J., J.S. Ojo, M.O. Olorunfemi. 2010. "Geophysical Investigation of Pavement Failure in a Basement Complex Terrain of Southwestern Nigeria". *Pacific Journal of Science and Technology*. 11(2):649-663.